

Further enhancement of light extraction efficiency of light-emitting diode with Ag film grown on photonic crystals

JIAN CHEN, QINGKANG WANG*, HAIHUA LI

National Key Laboratory of Micro/Nano Fabrication Technology,
Key Laboratory for Thin Film and Microfabrication Technology of Ministry of Education,
Research Institute of Micro/Nano Science and Technology,
Shanghai Jiao Tong University, Shanghai 200240, China

*Corresponding author: wangqingkang@sjtu.edu.cn

Photonic bandgap of photonic crystals (PCs) and the effect of grating diffraction can be used to improve the extraction efficiency of the light from a light-emitting diode (LED). The transmission of light at certain wavelength through periodic sub-wavelength hole arrays in metal films is extraordinary, because the surface plasmon acts effectively. In this letter, PCs with the square lattice of cylinder unit cells are placed in GaN layer of GaN-based blue LED, and the silver film is plated on PCs. The finite-difference time-domain (FDTD) method is used to investigate the optical transmission; the results show that the extraction efficiency of the PC-assisted LED (PC-LED) is enhanced when the silver film is plated on the PCs under certain conditions. Finally, we use the surface plasmon dispersion relation to analyze the mechanism of antireflection.

Keywords: photonic crystal, photonic bandgap, light-emitting diode, surface plasmon, transmission.

1. Introduction

GaN-based light-emitting diodes (LEDs) with a long life-cycle have been employed for various applications, such as large full-color displays, traffic signals, back light units for liquid-crystal display and so forth. Also it makes all-solid-state lighting a viable option for large-scale energy savings. Due to the index difference between air and a typical semiconductor which is used in LEDs, most spontaneously emitted waves undergoes total internal reflection at the interface of the LED medium and air and thus most of the emitted light remains trapped in the LED [1, 2]. In conventional structures, the extraction efficiency at the semiconductor/air single interface is approximately $1/4n^2$, where n is the refractive index of a semiconductor, at best, only about 5% of the light emitted is extracted from the top surface. Therefore, the issue is how to increase the amount of light extracted from an LED.

Many interesting approaches have been proposed to accomplish this, such as the use of thin light-emitting layers with surface texturing, resonant cavities, photon recycling, or output coupling through surface plasmons excited at corrugated metal surfaces. In recent years, many investigations use the wave nature of light, like photonic crystals (PCs) to enhance light extraction [3–6], which has been demonstrated and applied. Based on the photonic band gap (PBG) effect and coherent diffraction, the light output of PC-assisted LED (PC-LED) has been enhanced.

Due to the surface plasmons (SPs) effect, the transmission of light at certain wavelength through periodic sub-wavelength hole arrays in metal films is extraordinary [7–9]. In this paper, to further enhance the extraction efficiency of GaN-based blue LED, PCs with square lattice of cylinder unit cells are placed in GaN layer of GaN-based blue LED, and the silver film is plated only on the PCs, so we can use both the PBG effect and the SPs effect. We use the finite-difference time-domain (FDTD) method to investigate the optical transmission. First, we find out the best structure parameters of the PCs without Ag film, then we find out the best thickness of the Ag film for further enhancement.

2. Features of surface plasmon

SPs are free electron density oscillations on the surface of metals in dielectric materials. The propagation of a surface plasmon is always coupled with a surface electromagnetic wave along the metal–dielectric boundary [7]. QIU [10] has analyzed the enhanced effect of such transmission, pointing out two mechanisms: the localized surface plasmon waveguide resonance and the surface plasmon tunnel resonance, and discussed the two waveguide resonance frequencies starting from the band structure and the dispersion relations. WEN-HUNG CHUANG *et al.* [11] has demonstrated the differentiation between the contributions of localized surface plasmon (LSP) and surface plasmon polariton (SPP) couplings with an emitting dipole to emission enhancement in a metallic grating structure. In general, when light field incident with the cyclical structure of the metal, if the momentum and energy meet the conservation of energy, the incident light field can stimulate the plasma on the surface of metal. The plasma from the surface of a metal passes through the air hole tunneling to another surface and then releases photons. If the metal and dielectric materials are both semi-infinite, from the boundary solving Maxwell's equations, the dispersion relation of SPs can be determined as [12]

$$k_{\text{SP}} = k_0 \sqrt{\frac{\epsilon_d \epsilon_m}{\epsilon_d + \epsilon_m}} \quad (1)$$

where k_{SP} is the wave vector of the surface plasmon, ϵ_m and ϵ_d are the permittivity of the metal and dielectric material, which must have opposite signs if SPs are to be possible at such an interface. This condition is satisfied for metals because ϵ_m is both negative and complex. After calculation, $k_{\text{SP}} > k_0$, which shows that SP leads to a near-

-field enhancement. This increase in momentum is associated with the binding of the SP to the surface, and the resulting momentum mismatch between light and SPs of the same frequency must be bridged if light is to be used to generate SPs [12]. There are three main techniques by which the missing momentum can be provided [7]. The first makes use of prism coupling to enhance the momentum of the incident light. The second involves scattering from a topological defect on the surface, such as a sub-wavelength protrusion or hole, which provides a convenient way to generate SPs locally. The third makes use of a periodic corrugation in the metal's surface.

3. Design and modeling

Although the 3D-FDTD method enables us to acquire accurate results for the small size model structure, the large-area GaN-based blue LED cannot be treated faithfully because of the limited memory size. The structure of GaN-based blue LED is shown in Fig. 1. In this letter, PCs structures with a square lattice of cylinder unit cells are placed in the GaN layer (refractive index $n = 2.4$). The structure parameters of PCs: the period of PCs is a , the filling factor is $R_p = 2r/a$ (r is the radius of PCs), and the thickness of GaN layer is 300 nm.

The bandgap structure of 2D-PCs with the change of R_p is shown in Fig. 2. The number of the bandgaps with different R_p can be seen in Fig. 2a. When $R_p = 0.7$ the number of the bandgap is the largest. There are four bandgaps (Fig. 2b), two TE wave bandgaps: 0.315–0.346, 0.527–0.573, two TM wave bandgaps: 0.709–0.735, 0.89–0.904. The bandgap width is 0.031, 0.046, 0.026, 0.014(a/λ), respectively, so the center frequency f_0 is 0.33, 0.55, 0.722, 0.897(a/λ). As the light-emitting center wavelength is 460 nm, the period of PCs $a = f_0 \lambda = 151.8$ nm, 253 nm, 332.12 nm, 412.62 nm, thus we take $a = 412$ nm, $R_p = 0.7$. The 2D bandgap structure cannot be applied directly to 3D slab structure: the center frequencies are shifted toward the lower frequencies, thus the period of the PCs is an estimated value, but it has a direct reference value, and we will calculate the period later. When $a = 412$ nm, $R_p = 0.7$, the relation between the enhancement factor of extraction efficiency E_r of LED and the height of

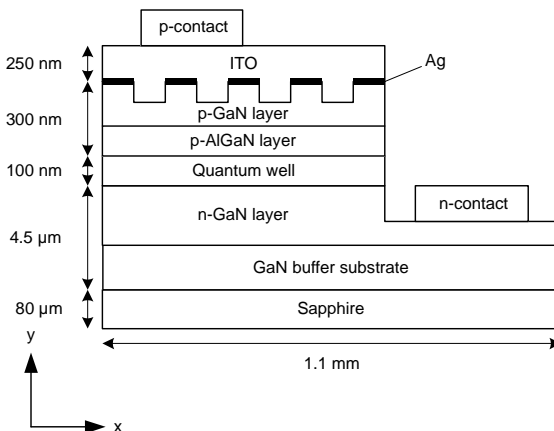


Fig. 1. The structure of GaN-based blue LED.

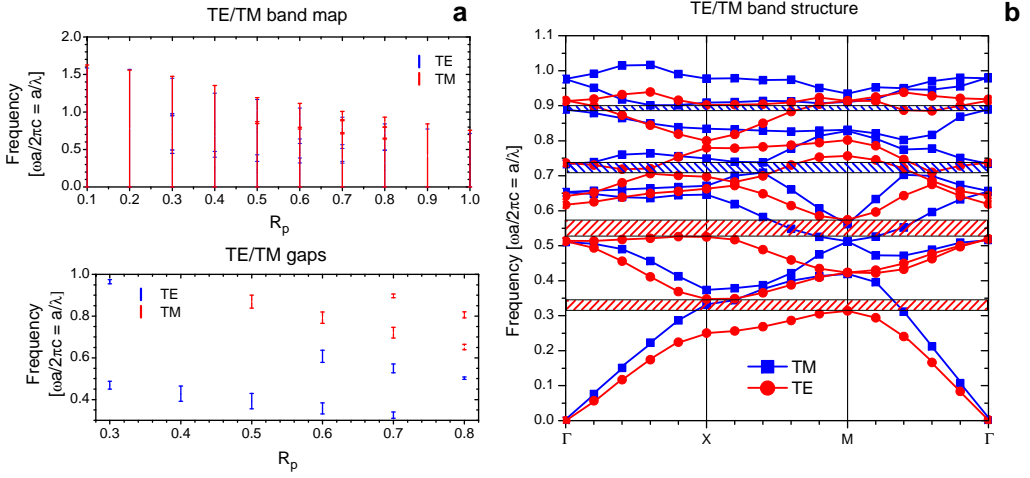


Fig. 2. The bandgap structure of PCs with different R_p (a); the PBG of PCs when $R_p = 0.7$ (b).

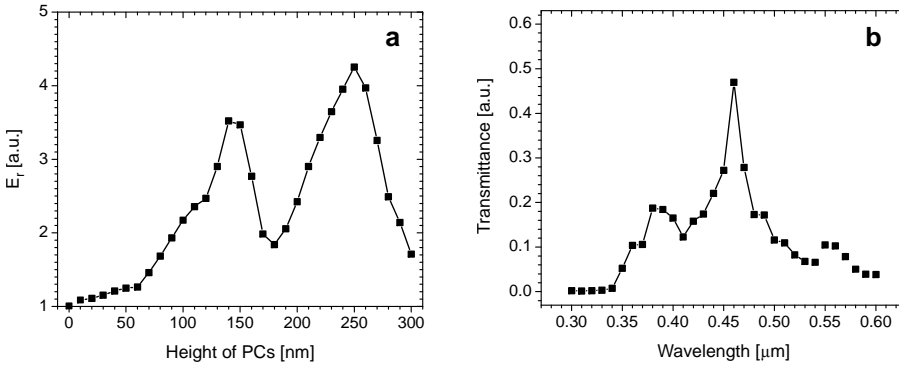


Fig. 3. The relationship between E_r and $\text{height}_{\text{PCs}}$ when $a = 412$ nm, $R_p = 0.7$ (a); the transmittance of the PCs when $a = 412$ nm, $R_p = 0.7$, $\text{height}_{\text{PCs}} = 250$ nm (b).

the PCs is shown in Fig. 3a. When $\text{height}_{\text{PCs}} = 250$ nm, the extraction efficiency is the largest – it is enhanced 3.3 times. Under the same conditions, the transmittance at 460 nm wavelength of the PCs is the highest (Fig. 3b).

For the two-dimensional symmetrical sub-wavelength structure of the increase in transmission, there are several formulas of the equivalent refractive index (n_{2D}) as follows [13]:

$$n_{2D}^2 = (1-f)n_i^2 + fn_s^2 \quad (2)$$

$$n_{2D}^2 = \frac{\left[(1-f)n_i^2 + fn_s^2 \right] \left[fn_i^2 + (1-f)n_s^2 \right] + n_i^2 n_s^2}{2 \left[fn_i^2 + (1-f)n_s^2 \right]} \quad (3)$$

$$(1 - f) \frac{n_s^2 - n_i^2}{n_s^2 - n_{2D}^2} = \frac{n_i}{n_{2D}} \quad (4)$$

where n_i is the refractive index of the medium, n_s is the refractive index of the substrate ($n_s = 2.4$), f is the area ratio of the substrate, here $f = 0.25\pi R_p^2$. The Eq. (2) is very different from the coupled-wave theory, the Eq. (3) matches the coupled-wave theory well when $n_s < 1.5$, the Eq. (4) matches the coupled-wave theory well when $1.5 < n_s < 4$. So we choose the Eq. (4) and get $n_{2D} = 1.347$. According to the film theory, when the thickness of the film $h = (2m + 1)\lambda_0/4n_{2D}$, the reflectivity is the smallest and the transmittance is the highest. When $m = 1$, $h = 256$ nm, which is in line with the result of Fig. 3.

We fix $R_p = 0.7$, $\text{height}_{\text{PCs}} = 250$ nm, to further enhance the extraction efficiency η of GaN-based blue LED. In this letter, the metal silver film was grown on the PCs, using the effect of SPs enhanced transmission to improve the efficiency. In this regard, a metallic grating structure is useful for phase matching of SP mode and radiation mode [11, 14]. The x - y plane distribution of the refraction of the FDTD simulation model is shown in Fig. 4b. For simplicity, the substrate is ignored in the model. From Fig. 4b, the real part of the refractive index of Ag is 0.0428 at wavelength of 460 nm, and $n_{\text{GaN}} = 2.4$, $n_{\text{ITO}} = 2$.

A three-dimensional FDTD method with a perfectly matched layer (PML) ($0.5 \mu\text{m}$) and periodic boundary condition (PBC) is carried out to simulate the optical properties of the presented PC-LED, providing a basis for the design of high-performance GaN-based blue LED. We intercept the region on x - y - z plane as $3 \times 3 \times 3$ (μm) and

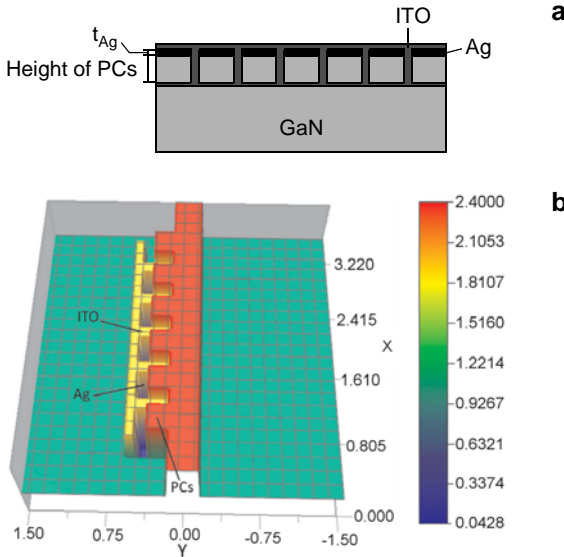


Fig. 4. The FDTD simulation model of the LED structure (a); the x - y plane distribution of the refraction index of the simulation model (b).

the grid size is 5 nm in all three dimensions. At the place $y = -1.5 \mu\text{m}$, we put continued guided-wave as an emitter source with its vacuum wavelength of 460 nm. The simulations are done for both polarizations, transverse electric (TE) and transverse magnetic (TM). Each calculation cell is setup repeatedly. The conductance of the ITO layer is ignored in the calculation, but it has no influence on SPs, and also can excite SPR [15, 16].

In order to model the plasmonic response, the complex dielectric constant of metal at optical frequencies is approximated by the Drude model as follows [17]:

$$\varepsilon(\omega) = \varepsilon_{\infty} - \frac{\omega_p^2}{\omega^2 + i\gamma\omega} \quad (5)$$

where ω is the light frequency, ω_p is the plasma frequency, γ is the damping frequency, $\omega_p = 1.3 \times 10^{16}$ rad/s, $\gamma = 4.6 \times 10^{13}$ rad/s [18]. When the incident light wavelength is 460 nm, $\omega = 4.1 \times 10^{15}$ rad/s.

4. Results and analysis

Based on the above analysis, we discuss the period of the PCs and the thickness of the Ag film which have influence on the extraction efficiency. In Fig. 5, when $t_{\text{Ag}} = 0$, $R_p = 0.7$ and $a = 410$ nm, the extraction efficiency η of PC-LED is the largest. The extraction efficiency becomes largest when the lattice constant is similar to the vacuum wavelength [19]. Enhancement of light extraction using 2D-PCs is achieved in two major schemes. The mechanism of light extraction enhancement is mainly related to the bandgaps of PCs. First, the bandgaps may be used to forbid

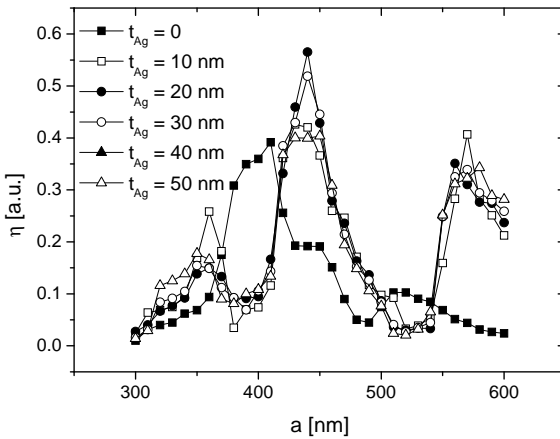


Fig. 5. When $R_p = 0.7$, the extraction efficiency as a function of a and t_{Ag} .

the emission into guided modes, PCs may be used to match the trapped waveguide modes within the LED to the bandgap of the PCs. The waveguide light thus lies within the bandgap of the PC, blocking its propagation in lateral directions within the structure, leaving only the external emission channel for light to exit the device. The second possibility is to utilize the refractive index periodicity of a PC to diffract waveguide modes above a certain cut-off frequency into externally propagating modes [1, 20–23]. The normalized frequency (a/λ) corresponding to our PCs structure ($a = 410$ nm, $R_p = 0.7$) is 0.891; only the TM modes lie in the bandgap region, TM modes can only radiate outward. But the gap width of TM modes is relatively narrow and TE modes lie below the cutoff frequency, so extraction enhancement in our LEDs is mainly due to coupling to leaky modes by Bragg diffraction as discussed earlier.

When the Ag film is grown on the PCs with $R_p = 0.7$ height_{PCs} = 250 nm, the extraction efficiency of PC-LED is the largest, on condition that $a = 440$ nm, $t_{Ag} = 20$ nm, which increases by 43.9% compared with the efficiency without the Ag film. Because t_{Ag} is small, the incident light does not constitute a complete reflection. Some of the energy permeates through the metal film, and some light wave oscillates in resonance with the SPs, so the transmission is enhanced. The surface plasmons help to confine the light intensity to the space behind the metal mask aperture by coupling [20]. The above mechanism is SPR. SPR is the resonance coupling between the incident light and the surface plasmon wave (SPW), it can lead to the transmission enhancement. With the increase in t_{Ag} , the extraction efficiency is reduced. This is because when t_{Ag} becomes larger, the absorption and reflection are strengthened. The propagation of a surface plasmon is always coupled with a surface electromagnetic wave along the metal–dielectric boundary.

The distribution of the magnetic field H_z of the designed LED is shown in Fig. 6. When $a = 440$ nm, $R_p = 0.7$, and $t_{Ag} = 20$ nm, the SPR effect is more obvious and the strength of the magnetic field H_z outside the PC-LED is higher than that when $a = 440$ nm, $R_p = 0.7$, and $t_{Ag} = 50$ nm.

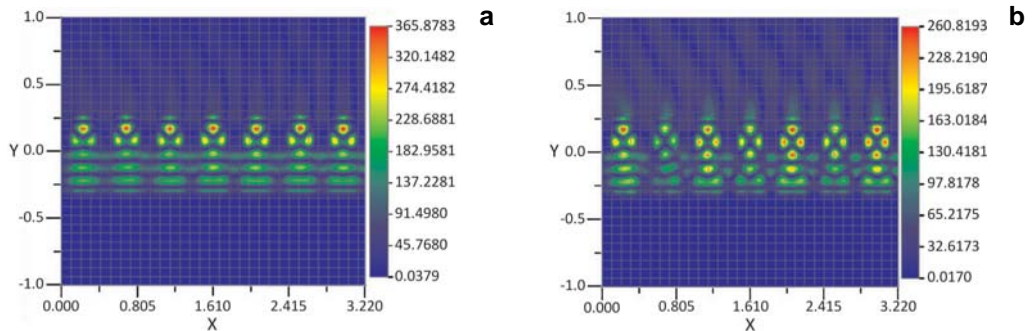


Fig. 6. The distribution of the magnetic field H_z of the designed LED with the same a and R_p , and: $t_{Ag} = 50$ nm (a), $t_{Ag} = 20$ nm (b).

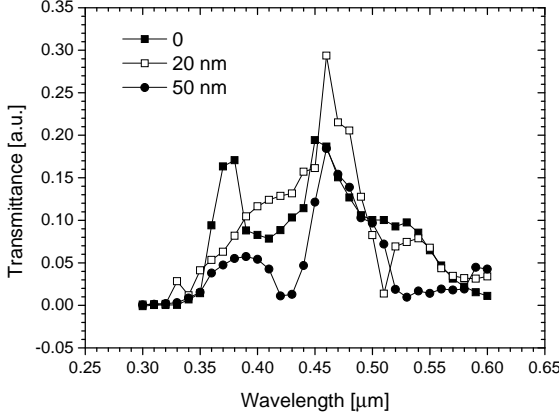


Fig. 7. Transmittance of the LED with the same a , R_p , and $\text{height}_{\text{PCs}}$ but with different t_{Ag} .

In general, photons will be lost from the semiconductor by the escape through the film top surface. The loss rate by the escape through the top surface is [24]:

$$\int_0^{\theta_c} dA \int B_{\text{int}} T(\theta) 2\pi \cos(\theta) \sin(\theta) d\theta = \frac{\pi B_{\text{int}} A \bar{T}}{n^2} \quad (6)$$

where B_{int} is the internal brightness in photons, θ is the polar angle, A is the surface area, θ_c is the critical escape angle, \bar{T} is the angle averaged transmission, and $T(\theta)$ is the transmission of the incident angle θ . The higher the transmittance, the larger the light extraction efficiency.

Figure 7 is the transmittance of the designed LED structure. When $a = 440$ nm, $R_p = 0.7$, $t_{\text{PCs}} = 250$ nm, and $t_{\text{Ag}} = 20$ nm, the transmittance at the wavelength around 460 nm is the highest, which is in line with the results above mentioned.

The SP resonances take place at around the positions of band edges. According to Eq. (1), the SP dispersion relations are as follows [25]:

$$k_{\text{SP}} = k_0 \left(\frac{\epsilon_m \epsilon_d}{\epsilon_m + \epsilon_d} \right)^{1/2} = n \frac{\pi}{a}, \quad (n = 1, 2, \dots) \quad (7)$$

$k_{\text{SP}} = 2\pi/\lambda_{\text{SP}}$, $\lambda_{\text{SP}} = \lambda_0 / [\epsilon_m \epsilon_d / (\epsilon_m + \epsilon_d)]^{1/2}$ is the wavelength of SP wave, λ_0 is the vacuum wavelength. For a square array at normal incidence, the transmission wavelength λ_{SP} is given by [26]

$$\lambda_{\text{SP}} = \frac{a}{(m^2 + n^2)^{1/2}} \cdot \left(\frac{\epsilon_m \epsilon_d}{\epsilon_m + \epsilon_d} \right)^{1/2} \quad (8)$$

where m and n are integers that correspond to the particular order of the SPP. According to the Eq. (5), when the center wavelength of the incident light is 460 nm, $\epsilon_{\text{Ag}} = -8.63 + 0.25i$, according to the Eq. (8), when $m^2 + n^2 = 16$, $\lambda_{\text{SP}} = 457.8$ nm ($\epsilon_{\text{GaN}} = 5.76$), which is closed to the center light-emitting wavelength of GaN-based blue LED. Therefore, the SPs could lead to the enhanced transmission at $\lambda_{\text{SP}} = 457.8$ nm because of the SPR, and the extraction efficiency of the GaN-based blue LED is enhanced.

The introduction of PCs can provide a bandgap in the dispersion relation of the guided modes at the frequency of emission, and the periodic corrugation of the Ag film can provide a bandgap for the TM_1 coupled SPP mode and the lowest-order TE mode. If we label the modes by the effective index of the PCs $n_{2\text{D}}$, low-order modes ($n_{\text{GaN}} - 0.15 < n_{2\text{D}} < n_{\text{GaN}}$) are mostly localized in the core of the GaN waveguide and barely overlap with the PCs, leading to poor diffraction efficiency. On the other hand, high-order modes ($n_{\text{sapphire}} < n_{2\text{D}} < n_{\text{GaN}} - 0.15$) acquire a better extraction rate [27]. From Eq. (4), the $n_{2\text{D}} = 2.14$ (here $n_i = n_{\text{ITO}} = 2$), which satisfied the high-order modes.

5. Conclusions

Without PCs, guided modes will exist in the whole frequency. With the introduction of PCs, it will introduce a limit of guided wave frequency which reduces the guided modes and increases the leaky modes. When Ag film was grown on the PCs, the extraction efficiency of PC-LED is further enhanced under certain conditions. The resonance coupling occurs between the incident light and the SPW inspired on the metal surface and the resonance wavelength is 457.8 nm, so the SPR leads to the enhanced transmission.

Acknowledgements – This research was supported by the Shanghai Committee of Science and Technology of China (Grant No. 0752nm014) and the National Natural Science Foundation of China (Grant No. 60808014).

References

- [1] DAVID A., BENISTY H., WEISBUCH C., *Optimization of light-diffracting photonic-crystals for high extraction efficiency LEDs*, Journal of Display Technology **3**(2), 2007, pp. 133–148.
- [2] XIANGSU ZHANG, SHOU LIU, YING LIU, XIAOYUN CHEN, HAN LIN, XUECHANG REN, *Enhancement of LED light extraction via diffraction of hexagonal lattice fabricated in ITO layer with holographic lithography and wet etching*, Physics Letters A **372**(20), 2008, pp. 3738–3740.
- [3] BORODITSKY M., KRAUSS T. F., COCCIOLI R., VRIJEN R., BHAT R., YABLONOVITCH E., *Light extraction from optically pumped light-emitting diode by thin-slab photonic crystals*, Applied Physics Letters **75**(8), 1999, pp. 1036–1038.
- [4] SZYMANSKA M.H., HUGHES A.F., PIKE E.R., *Effect of a photonic band gap on the threshold and output power of solid-state lasers and light-emitting diodes*, Physical Review Letters **83**(1), 1999, pp. 69–72.
- [5] FAN S.H., VILLENEUVE P.R., JOANNOPOULOS J.D., *Rate-equation analysis of output efficiency and modulation rate of photonic crystal light-emitting diodes*, IEEE Journal of Quantum Electronics **36**(10), 2000, pp. 1123–1130.

- [6] MATTERSON B.J., LUPTON J.M., SAFONOV A.F., SALT M.G., BARNES W.L., SAMUEL I.D.W., *Increased efficiency and controlled light output from a microstructured light-emitting diode*, *Advanced Materials* **13**(2), 2001, pp. 123–127.
- [7] EBBESEN T.W., LEZEC H.J., GHAEMI H.F., THIO T., WOLFF P.A., *Extraordinary optical transmission through subwavelength hole arrays*, *Nature* **391**(6668), 1998, pp. 667–669
- [8] LEZEC H.J., DEGIRON A., DEVAUX E., LINKE R.A., MARTIN-MORENO L., GARCIA-VIDAL F.J., EBBESEN T.W., *Beaming light from a subwavelength aperture*, *Science* **297**(5582), 2002, pp. 820–822.
- [9] THIO T., PELLERIN K.M., LINKE R.A., LEZEC H. J., EBBESEN T.W., *Enhanced light transmission through a single subwavelength aperture*, *Optics Letters* **26**(24), 2001, pp. 1972–1974.
- [10] QIU M., *Photonic band structures for surface waves in structured metal surfaces*, *Optics Express* **13**(19), 2005, pp. 7583–7588.
- [11] WEN-HUNG CHUANG, JYH-YANG WANG, YANG C.C., YEAN-WOEI KIANG, *Differentiating the contributions between localized surface plasmon and surface plasmon polariton on a one-dimensional metal grating in coupling with a light emitter*, *Applied Physics Letters* **92**(13), 2008, p. 133115.
- [12] BARNES W.L., DEREUX A., EBBESEN T.W., *Surface plasmon subwavelength optics*, *Nature* **424**(6950), 2003, pp. 824–830.
- [13] RAGULN D.H., *Subwavelength Structured Surfaces: Theory and Application*, The University of Rochester, USA, 1993.
- [14] WEN-HUNG CHUANG, JYH-YANG WANG, YANG C.C., YEAN-WOEI KIANG, *Numerical study on quantum efficiency enhancement of a light-emitting diode based on surface plasmon coupling with a quantum well*, *IEEE Photonics Technology Letters* **20**(16), 2008, pp. 1339–1341.
- [15] JIN-A JEONG, HAN-KI KIM, *Low resistance and highly transparent ITO–Ag–ITO multilayer electrode using surface plasmon resonance of Ag layer for bulk-heterojunction organic solar cells*, *Solar Energy Materials and Solar Cells* **93**(10), 2009, pp. 1801–1809.
- [16] SZUNERITS S., CASTEL X., BOUKHERROUB R., *Surface plasmon resonance investigation of silver and gold films coated with thin indium tin oxide layers: Influence on stability and sensitivity*, *Journal of Physical Chemistry C* **112**(40), 2008, pp. 15813–15817
- [17] PALIK E.D., *Handbook of Optical Constants in Solids*, Academic, New York, 1998.
- [18] QUONG M.C., ELEZZABI A.Y., *Offset-apertured near-field scanning optical microscope probes*, *Optics Express* **15**(16), 2007, pp. 10163–10174.
- [19] YONG-JAE LEE, SE-HEON KIM, JOON HUH, GUK-HYUN KIM, YONG-HEE LEE, SANG-HWAN CHO, YOON-CHANG KIM, YOUNG RAG DO, *A high-extraction-efficiency nanopatterned organic light-emitting diode*, *Applied Physics Letters* **82**(21), 2003, pp. 3779–3781.
- [20] LONČAR M., DOLL T., VUČKOVIĆ J., SCHERER A., *Design and fabrication of silicon photonic crystal optical waveguides*, *Journal of Lightwave Technology* **18**(10), 2000, pp. 1402–1411.
- [21] ADAWI A.M., KULLOCK R., TURNER J.L., VASILEV C., LIDZEY D.G., TAHRAOUI A., FRY P.W., GIBSON D., SMITH E., FODEN C., ROBERTS M., QURESHI F., ATHANASSOPOULOU N., *Improving the light extraction efficiency of polymeric light emitting diodes using two-dimensional photonic crystals*, *Organic Electronics* **7**(4), 2006, pp. 222–228.
- [22] ODER T.N., KIM K.H., LIN Y.J., JIANG H.X., *III-nitride blue and ultraviolet photonic crystal light emitting diodes*, *Applied Physics Letters* **84**(4), 2004, pp. 466–468.
- [23] NG W.N., LEUNG C.H., LAI P.T., CHOI H.W., *Photonic crystal light-emitting diodes fabricated by microsphere lithography*, *Nanotechnology* **19**(25), 2008, p. 255302.
- [24] SCHNITZER I., YABLONOVITCH E., CANEAU C., GMITTER T.J., SCHERER A., *30% external quantum efficiency from surface textured, thin-film light-emitting diodes*, *Applied Physics Letters* **63**(16), 1993, pp. 2174–2176.
- [25] ZHIJUN SUN; DANYAN ZENG, *Modeling optical transmission spectra of periodic narrow slit arrays in thick metal films and their correlation with those of individual slits*, *Journal of Modern Optics* **55**(10), 2008, pp. 1639–1647.

- [26] YI-TSUNG CHANG, DAH-CHING TZUANG, YI-TING WU, CHI-FENG CHAN, YI-HAN YE, TING-HSIANG HUNG, YU-FAN CHEN, SI-CHEN LEE, *Surface plasmon on aluminum concentric rings arranged in a long-range periodic structure*, Applied Physics Letters **92**(25), 2008, p. 253111.
- [27] DELBEKE D., BIENSTMAN P., BOCKSTAELE R., BAETS R., *Rigorous electromagnetic analysis of dipole emission in periodically corrugated layers: The grating-assisted resonant-cavity light-emitting diode*, Journal of the Optical Society of America A **19**(5), 2002, pp. 871–880.

*Received June 7, 2010
in revised form August 23, 2010*